FACULTY OF CIVIL ENGINEERING RIJEKA

UNIVERSITY OF RIJEKA

UKF Project 3/13

Evidence Based Characterisation of Dynamic Sensitivity for Multiblock Structures - Computational Simulation and Experimental Validation

PROJECT REPORT 1

Nina Čeh

Rijeka, January 2014

Contents

View of the project plan

Key performance indicator	1st half-year	2nd half-year	3rd half-year	4th half-year
Literature Review (benchmarks)	**Single block**	**Multi-block configuration**	/	/
Experiments	Single block	Stack of blocks	Multiple stacks of blocks	Complex assemblies
Computational Simulation and Validation	Single block ("benchmarks")	Stack of blocks	Multiple stacks	Complex assemblies
Dynamic Characterisation	Single block	Stack of blocks	/	Multiple stacks

1. Introduction

Multiple rigid body system response to dynamic excitation differs from the response of deformable structural systems. For multi body system, no eigenvalue problem can be formulated, therefore it is not possible to characterize its dynamic behaviour in the same way as the characterization can be defined for deformable bodies. When it comes to safety assessment for such structures during an earthquake or other dynamic excitations, there are very few or no clear instructions or guidelines. The main aim of this project is to attempt to characterize dynamic behaviour of multiple rigid block structures and validate several simulation frameworks.

This first report looks reviews the available set of benchmark problems, single block structures or assemblies of simple multiple rigid blocks, for which some idealised analytical solutions can be formulated. This report responds to the initial part of the work plan, associated with the development of a series of single and multi block benchmarks and experimentally validation of their response.

Based on basic characteristics of the system considered, every problem will be identified according to scheme as stated in Table 1.

Table 1. Problem characterization codes based on characteristics of the system and excitation

TYPE OF STRUCTURE		TYPE OF CONTACT		CONSTRAINTS		EXCITATION	
S	Single block	**RO**	Rocking only	**C**	Any type of constraints	**F**	Free rocking
D	Double block (Bi-block)	**RS**	Rocking and sliding	**O**	No constraints	**H**	Harmonic excitation
M	Multiple blocks					**G**	General excitation

In the subsequent discussion, for every problem considered for illustration or comparison purposes, a reference has been made to specific papers (marked always by a box), and by indicating principal issues of importance for the current project.

Moreover, in the following sections, predictions of a developed in house MATLAB code is have been frequently illustrated, validated and/or compared to a number of benchmark problems published in literature.

2. Single rigid block

2.1. Free rocking of a single rigid block

A single rigid block resting on a ground is capable of rocking when excited by ground motion. The friction between block and ground is considered to be large enough to prevent any sliding. Block is defined by its width B, height H and mass m. For an isotropic block it is easy to define the position of its centre of mass $C.M.$ Angle of slenderness α is defined by block's geometry. An example of a single rigid block is shown on Figure 1.

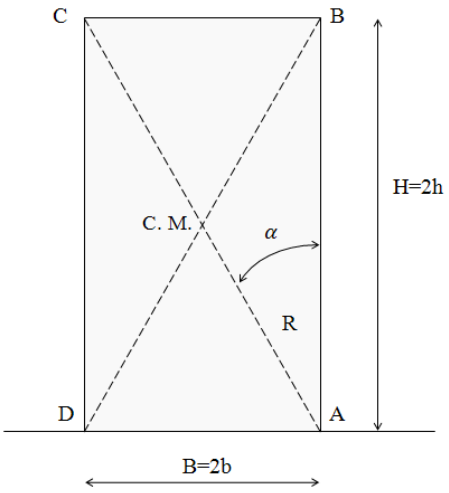

Figure 1. Single rigid block structure with displayed geometric characteristics

Edges of rigid block are used to describe its motion. When suspended from an initial clockwise rotation, the block tends to return to the position of its static equilibrium due to its weight. For this reason block starts to rotate counter-clockwise, which is defined as negative angular movement about the edge corner A.

Basic equation of motion (EOM) used to describe motion of single rigid block with no excitation (SROOF) is given (Housner, 1963):

$$I_0 \cdot \ddot{\theta} = -W \cdot R \cdot sin(sign(\theta) \cdot \alpha - \theta) \quad (1)$$

In the above equation I_0 is the mass moment of inertia, $\ddot{\theta}$ is the angular acceleration of the block with its 1st derivative angular velocity of the block $\dot{\theta}$ and 2nd derivative angular displacement or rotation θ, and W is the weight of the block.

Possible configurations of the block during free rocking without sliding between block and base are shown in Figure 2.

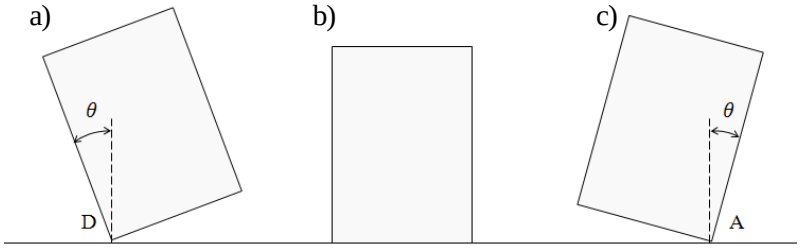

Figure 2. Possible configurations of single rigid block during rocking: a) counter-clockwise (negative) rotation; b) no rotation; c) clockwise (positive) rotation

From Figure 2 it is possible to note a non-smooth transition between the rotation about the edge A to the rotation about the edge D, defined by the rotation angle $\theta = 0°$. During this transition an impact between block and base occurs. Impact and transition between the two centres of rotation is what makes the dynamics of a single rigid block non-smooth and discontinuous.

An impact between the block and the base can be treated in many different ways. Early literature on this topic suggests treatment of impact as a perfectly elastic point impact augmented by a decrease of the angular velocity right after impact compared to the angular velocity just before impact. The ratio between these two velocities can be viewed as equivalent to the usual coefficient of restitution in normal impact.

Follwing Housner's classical paper (Housner, 1963), an alternative coefficient of restitution can be obtained from the condition for conservation of moment of momentum about the edge A (or D) during an impact:

$$I_0\dot{\theta}_1 - 2mRb\dot{\theta}_1 \sin\alpha = I_0\dot{\theta}_2 \tag{2}$$

which gives:

$$r = \left[1 - \frac{mR^2}{I_0}(1 - \cos 2\alpha)\right]^2 \tag{3}$$

where the coefficient of restitution defined this way represents a reduction in kinetic energy during impact:

$$r = \frac{\frac{1}{2}I_0{\dot{\theta}_2}^2}{\frac{1}{2}I_0{\dot{\theta}_1}^2} = \left(\frac{\dot{\theta}_2}{\dot{\theta}_1}\right)^2 \tag{4}$$

On the other hand, if the coefficient of restitution is defined as a reduction on angular velocity during impact (Dimitrakopoulos and DeJong, 2012):

$$\eta = \frac{\dot{\theta}_2}{\dot{\theta}_1} \tag{5}$$

Various authors arrive at different solutions for the value of this coefficient, but the most precise way is to experimentally determine the value for each combination of materials.

For slender blocks with small angle of slenderness the EOM given by eq. (1) can be justifiably linearised (Housner, 1963):

$$I_0 \cdot \ddot{\theta} = -W \cdot R \cdot (sign(\theta) \cdot \alpha - \theta) \tag{6}$$

The above linearised equation of motion implies that the rotations are also small, which is valid for relatively low amplitudes of excitation. If there is no excitation, the block will overturn when the condition of static equilibrium is violated, i.e. when the centre of mass reaches a position outside of the current centre of rotation and starts to increase overturning moment. That means that when the angle of block rotation θ is greater than angle of slenderness, the block will overturn if not excited by external excitation.

By modifying eq. (2) it is possible to identify a frequency like parameter, which depends only on geometry of the block for a rigid rectangular isotropic homogeneous block (Housner, 1963):

$$p = \sqrt{\frac{W \cdot R}{I_0}} = \sqrt{\frac{4R}{3g}} \tag{7}$$

The above equation indicates that rocking frequency is only related to geometry of the block. Period of rocking is then given as (Housner, 1963):

$$T = \frac{4}{p}\cosh^{-1}\left(\frac{1}{1 - {\theta_0}/{\alpha}}\right) \tag{8}$$

A very interesting point is that rocking period depends on a maximum rocking amplitude at the beginning of that period (Figure 3, Figure 4 and Figure 5).

The linearised equation of motion Eq. (2) was solved numerically using an ad-hoc Matlab code with both an explicit central difference method and implicit Newmark's method. The recursive scheme using Newmark's method has the form:

$$\theta_i = \frac{-\frac{WR\alpha\beta dt^2}{I_0} + \theta_{i-1} + dt\dot{\theta}_{i-1} + \left(\frac{1}{2} - \beta\right) dt^2 \ddot{\theta}_{i-1}}{1 - \frac{WR\beta dt^2}{I_0}} \tag{9}$$

In the above, the angular velocity and angular acceleration are given as:

$$\dot{\theta}_i = \dot{\theta}_{i-1} + (1-\gamma)dt\ddot{\theta}_{i-1} + \gamma dt\ddot{\theta}_i \tag{10}$$

$$\ddot{\theta}_i = \frac{\theta_i - \theta_{i-1} - dt\dot{\theta}_{i-1} - \left(\frac{1}{2} - \beta\right)dt^2\ddot{\theta}_{i-1}}{\beta dt^2} \tag{11}$$

In the above equations β and γ are Newmark's method parameters and dt is size of time step.

Results from the developed Matlab code were compared to the results in published literature.

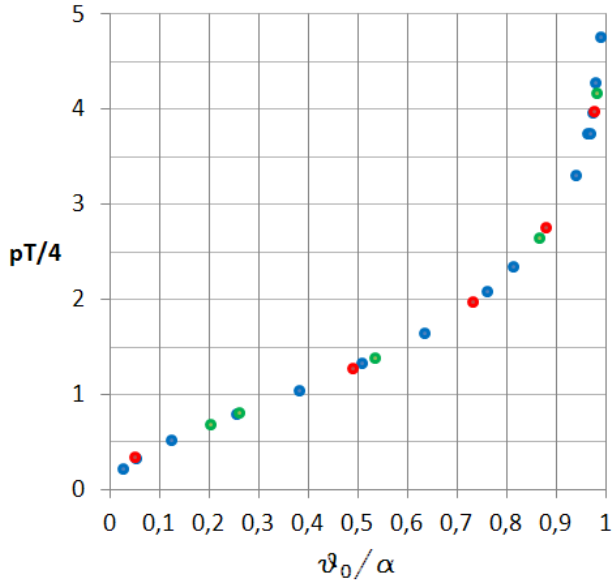

Figure 3. Period T of block rocking with amplitude θ_0 (according to Housner, 1963.)

Maxima of rocking amplitudes subsequent to the n-th impact of the block with the base (coefficient of restitution 0.7), from Housner's paper (Housner, 1963) are given on Figure 4.

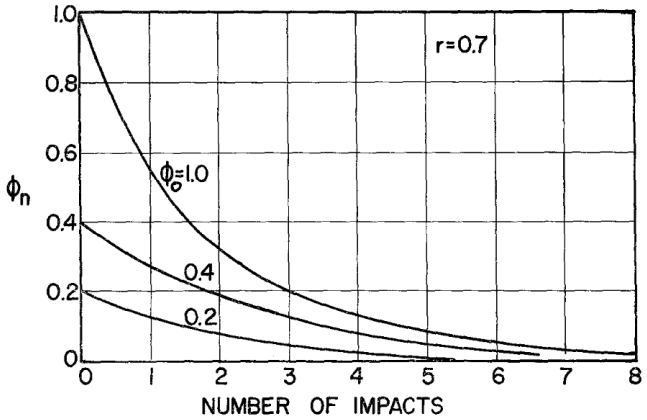

Figure 4. Rocking amplitude φ_n subsequent to n-th impact for coefficient of restitution r (Housner, 1963.)

Rocking amplitude subsequent to the n-th impact of block with the base defined by coefficient of restitution as reduction in angular velocity during impact from the current MATLAB code is given in Figure 5.

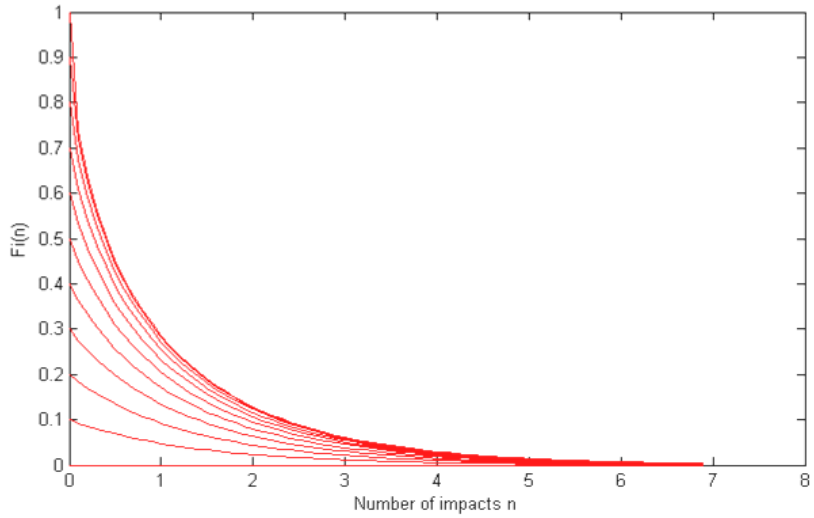

Figure 5. Amplitude subsequent to n-th impact for coefficient of restitution η =0.7 (according to Housner, 1963.)

When numerically solving the EOM, either the exact time of impact needs to be calculated or an approximation error occurring by letting the time of impact coincide with the time at the end of time step in which impact happened.

Literature review of 2.1. Free rocking of single rigid blocks	
Reference	**Conclusions**
Housner (1963)	*Frequency parameter* *Period duration* *Coefficient of restitution (r)* *Amplitude and duration for overturning by constant acceleration*
Dimitrakopoulos and DeJong (2012)	*Coefficient of restitution (η)*

2.2. Single rigid block under harmonic excitation

External base excitation in a form of constant ground acceleration with a sufficient intensity can rock a rigid block. Since this type of excitation has no equivalent in nature, the simplest type of excitation that should be discussed is harmonic excitation. A single wave of sine or cosine harmonic excitation can violate block's stability. Sine type excitation is given as:

$$\ddot{u}_g(t) = a_g \cdot \sin(\omega \cdot t + \psi) \tag{12}$$

In the above equation a_g is ground acceleration amplitude, ω is ground acceleration angular frequency and ψ is phase lag. In this case there is an additional parameter which affects block motion and the EOM is given as (Housner, 1963):

$$\begin{gathered} I_0\ddot{\theta} = -Wk_w - F_a k_a \\ I_0\ddot{\theta} = -WR\sin(sign(\theta)\cdot\alpha - \theta) - m\cdot\ddot{u}_g(t)\cdot R\cos(sign(\theta)\cdot\alpha - \theta) \end{gathered} \tag{13}$$

The principal interest is to define the condition for overturning of the block by such harmonic ground acceleration, also depending on the ground acceleration amplitude. Many authors tried to give exact expressions for overturning condition, but the main difficulty is a highly non-linear equation by which the overturning condition is defined. In the early years, authors defined the actual overturning as an angular displacement equal to the angle of slenderness of the block at the time instant when the ground acceleration expires. But, this condition proved to be insufficiently rigorous because the block can survive the forced rocking phase with displacements smaller than the angle of slenderness and overturn in the subsequent free rocking phase. The condition for such overturning is the existence of an extreme in angular velocity of the block graph: if the angular velocity curve is asymptotically approaching x-axis, but never actually reaches it, the block will overturn. Minimal value of the peak amplitude of ground acceleration is needed if the ground acceleration is high enough for the block to start rocking at the beginning, given as (Housner, 1963):

$$g\sin\alpha = a\sin\psi \tag{14}$$

Correct form of the above equation is:

$$g\frac{\sin\alpha}{\cos\alpha} = g\tan\alpha = a\sin\psi \tag{15}$$

The above condition in its linearised form can be expressed as (Makris and Rousses, 1998):

$$\cos\psi\cosh\left[\frac{p}{\omega_p}(\pi-\psi)\right] - \frac{\omega_p}{p}\sin\psi\sinh\left[\frac{p}{\omega_p}(\pi-\psi)\right] + 1 + \cos\psi\sinh\left[\frac{p}{\omega_p}(\pi-\psi)\right] - \frac{\omega_p}{p}\sin\psi\cosh\left[\frac{p}{\omega_p}(\pi-\psi)\right] = 0 \tag{16}$$

Since the exact solution of the above equation cannot be obtained analytically, the closest values can be arrived at through a numerical solution. The values of minimal peak ground acceleration for half of sine wave excitation, derived from approximate analytical expressions given by different authors and by numerically solving eq. (16) are given in Table 2. Numerical solution is obtained from an ad-hoc MATLAB code written using the Newmark's method for solving the differential EOM and compared to results by Housner and Makris.

Table 2. Minimal peak ground acceleration amplitude given in percents of gravitational acceleration

b	h	R	A	p	a_{g0}/g		
					(Housner, 1963)	(Makris and Rousses, 1998)	(Matlab)
0,20	0,60	0,6325	0,32175	3,4100	0,6745	0,6182	0,5547
0,25	0,75	0,7906	0,32175	3,0501	0,7368	0,6532	0,5884
0,30	0,90	0,9487	0,32175	2,7844	0,7942	0,6848	0,6194
0,40	1,20	1,2649	0,32175	2,4114	0,8980	0,7409	0,6748
0,45	1,35	1,4230	0,32175	2,2735	0,9456	0,7664	0,6999
0,50	1,50	1,5810	0,32175	2,1569	0,9910	0,7904	0,7238

Since the analytical expressions are approximate, it is to be expected that the obtained values will not satisfy eq. (16). Housner's solution is based on s completely different overturning condition so his values are expected to differ from zero the most. The values of left-hand side of eq. (16) are given in Table 3.

Table 3. Values of left-hand side of eq. (16)

b	h	(…) = 0		
		(Housner, 1963)	(Makris and Rousses, 1998)	(Matlab)
0,20	0,60	1,0000	0,5702	0,0005
0,25	0,75	1,0000	0,4828	-0,0036
0,30	0,90	1,0000	0,4249	-0,0035
0,40	1,20	1,0000	0,3516	-0,0027
0,45	1,35	1,0000	0,3267	-0,0027
0,50	1,50	1,0000	0,3063	-0,0020

Numerically gained values are more exact than the approximate solutions. Overturning condition given by eq. (16) is shown in Figure 6.

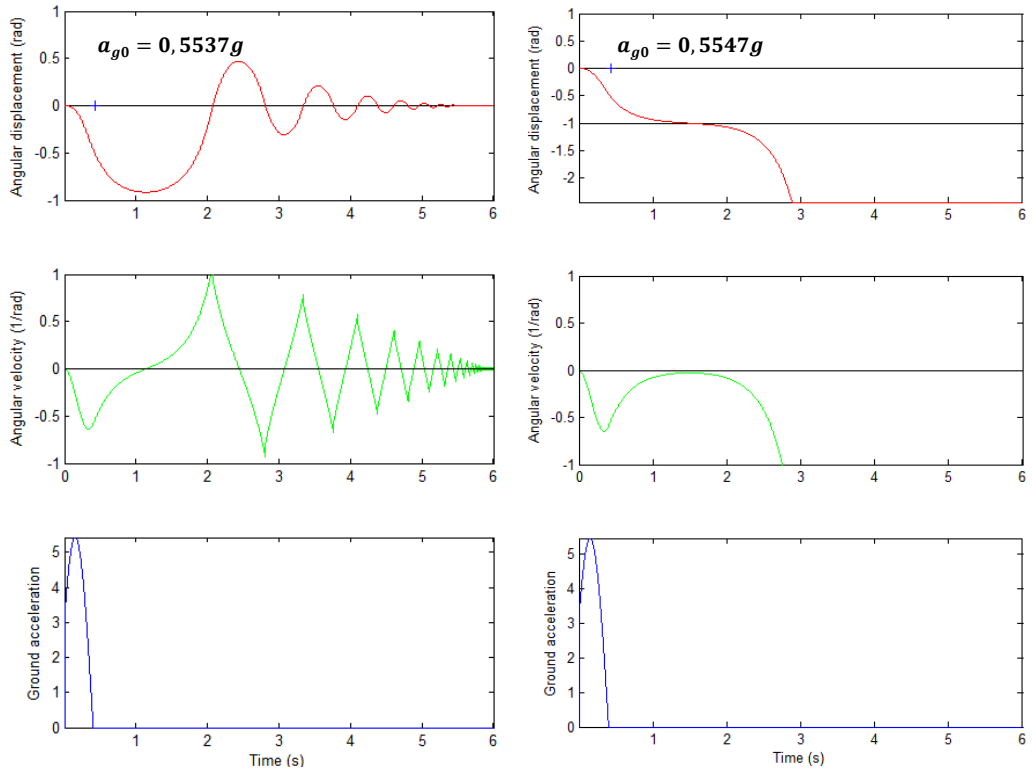

Figure 6. Rotation and angular velocity time histories of a rigid block subjected to two half-sine pulse excitations: no overturning (left) and overturning (right)

Strictly speaking, there is a need to distinguish three different "types" of overturning - **case 1.1** is defined by block surviving a single impact with base during the duration excitation and overturning after the excitation had expired; **case 1.2** is defined by the block surviving a single impact after the excitation had expired and then overturning; and the **case 2** is defined by the block overturning without an impact with base (Dimitrakopoulos and DeJong, 2012). Eq. (16) and approximate solutions deal with the overturning case 2.

By numerically solving eq. (15) for a single sine type excitation the curves that delineate the two overturning cases – the case 1.1 and overturning case 1.2 are gained (Figure 7).

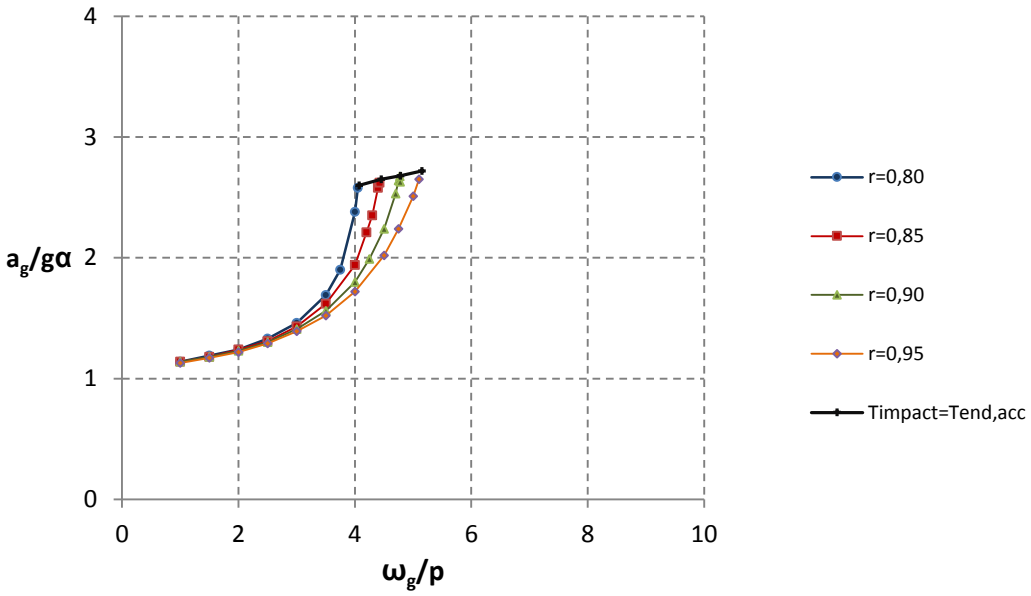

Figure 7. Curve that delineates overturning case 1.1 from overturning case 1.2 (black) and curves representing overturning condition for overturning case 1.1 for different values of coefficient of restitution

There have been many attempts to characterize dynamic behaviour of rigid blocks based on the geometric similarity, only about two years ago this was succeeded. An analysis was carried out using the Buckingham's theorem and the so called orientational analysis principles (Dimitrakopoulos and DeJong, 2012).

As a result, several dimensionless (and orientationless) groups of equations were derived (Dimitrakopoulos and DeJong, 2012), providing evidence of self-similarity in rocking response for slender and non-slender blocks.

Rotation and angular velocity time histories for two blocks of different shape and size are shown in Figure 8. By using the dimensionless-orientationless approach these curves for different blocks can be represented with one "master" curve. The results given in literature were compared and validated using the developed ad-hoc MATLAB code.

$b_1 = 0{,}024\ m$
$h_1 = 0{,}269\ m$
$R_1 = 0{,}27\ m$
$\alpha_1 = 5°$
$p_1 = 5{,}24\ rad/s$
$a_{g,1} = 1{,}2\ m/s^2$
$\omega_{g,1} = 2\pi/T_{g,1}$
$T_{g,1} = 0{,}60\ s$

$b_2 = 0{,}083\ m$
$h_2 = 0{,}473\ m$
$R_2 = 0{,}48$ m
$\alpha_2 = 10°$
$p_2 = 3{,}92\ rad/s$
$a_{g,2} = 2{,}4\ m/s^2$
$\omega_{g,2} = 2\pi/T_{g,2}$
$T_{g,2} = 0{,}80\ s$

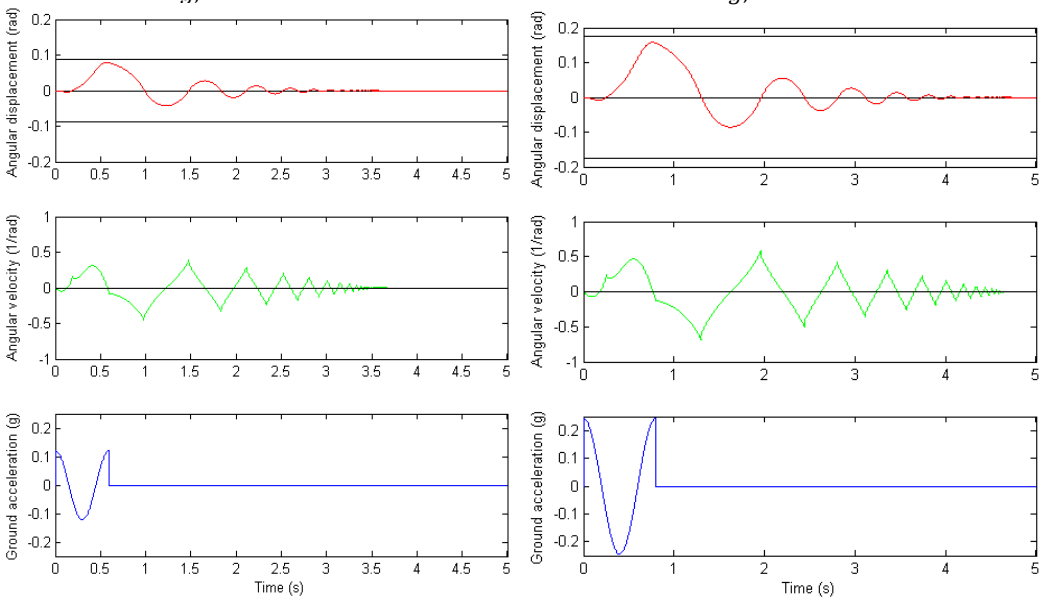

Figure 8. The response of two similar rocking blocks of different shape and size to a single cosine type acceleration

The axis has to be scaled to $\tau = tp$ and the angular displacement, angular velocity and ground acceleration are normalized by a_g/g , $a_g p/g$ and a_g, respectively. Time-histories obtained in that way are shown in Figure 9 and excellent agreement with the paper by Dimitrakopoulos and DeJong, 2012 is noted.

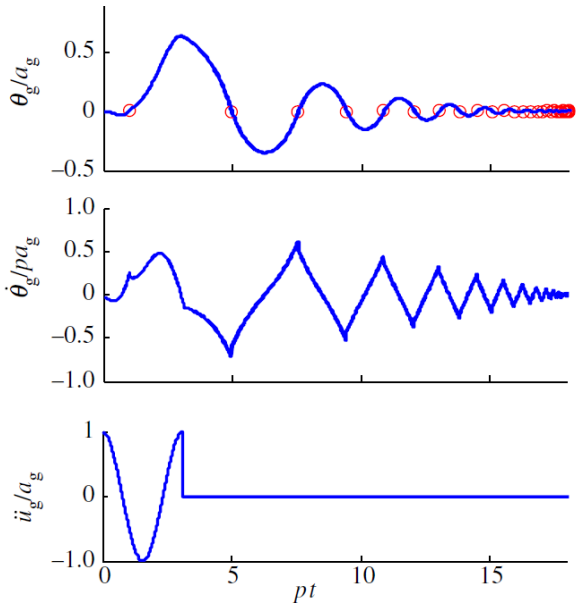

Figure 9. Dimensionless rotation, angular velocity and ground acceleration time-histories for two blocks of different shape and size (dimensionless time-history curves are equal) (Dimitrakopoulos and DeJong, 2012.)

The main goal of a great number of papers in this field is to determine whether a rigid block will overturn when excited by harmonic excitation of given frequency and amplitude. It transpires that there are values of excitation frequency where the block is expected to overturn (by experiencing an angular displacement greater than the value of angle of slenderness) but the block returns to a stable position. This is very counterintuitive and should be further researched. The cause for this manifestation stems from the fact that the ground acceleration starts acting in the opposite direction to x-axis projection of angular velocity of the block when $\theta \geq \alpha$. To clarify this behaviour simulations have been run to see if it is possible for block to recover from the apparent overturning more than once. Simulations were carried out using the developed ad-hoc MATLAB code, capable of counting a number of events when block passed through the threshold of the angle of slenderness and the number of events when the block returned to the area of stability. If the number of crossing beyond the overturning threshold is greater than the number of returns, the block eventually overturned. Otherwise the block remained stable. Example of the output graph is shown in Figure 10.

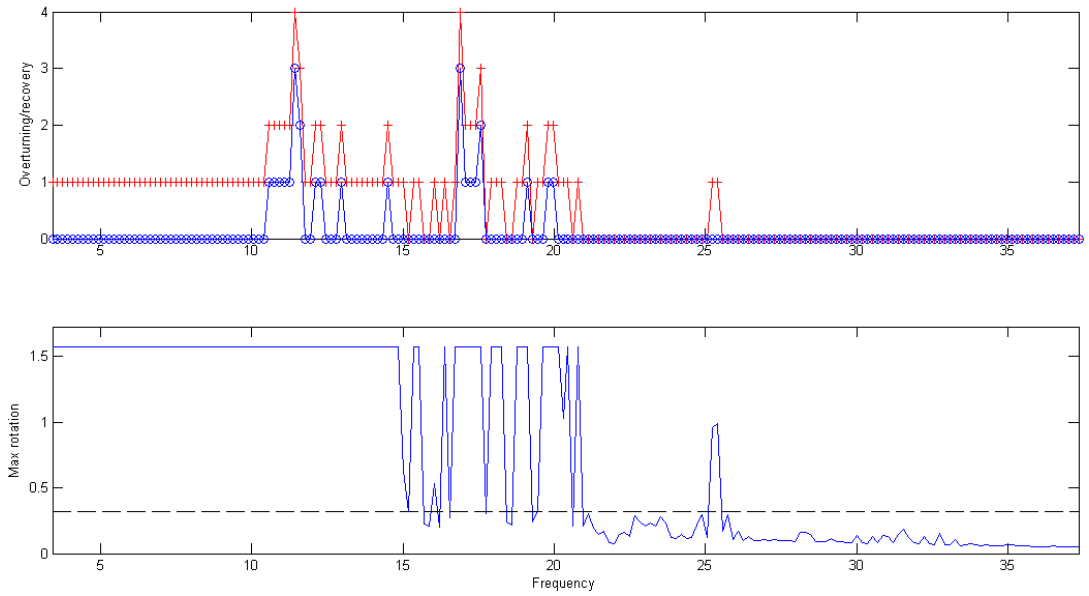

Figure 10. Overturning, recovery and stability of rigid block depending on the frequency of ground acceleration (for a fixed acceleration amplitude)

Although the results indicate that some values of excitation frequency can result in block recovery, it can be seen that for slightly lower and slightly greater values of excitation frequency block will overturn. For this reason events of block recovering from overturning are to be considered construction failures and equivalent to overturning.

Literature review for 2.2. Single rigid block under harmonic excitation	
Reference	**Conclusions**
Housner (1963)	*Minimal peak ground acceleration for overturning by sine wave ground acceleration*
Dimitrakopoulos and DeJong (2012)	*Transient dynamics* *Similarity laws from dimensional analysis and dimensionless graphs*
Makris and Rousses (1998)	*Minimal peak ground acceleration for overturning by half-sine wave acceleration (numerical and approximate analytic solution)*
Zhang and Makris (2001)	*Ground acceleration amplitude versus frequency for overturning (sine and cosine pulse)*
Anooshehpoor, Heaton, Shi and Brune (1999)	*Minimal peak ground acceleration for overturning*
Purvance, Anooshehpoor and Brune (2008)	*Peak ground acceleration for overturning of symmetric and asymmetric single blocks*

2.3. Hogan's analysis of rigid block motion

During the past two decades several authors (Hogan, Spanos) developed a slightly different approach to rigid block dynamics in rocking. The main thrust of their research moved from simply trying to define the overturning stability of rigid blocks to trying to better visualise and more fully understand their transient and steady-state dynamic behaviour.

This research suggests that the block reaching steady-state rocking can conveniently be viewed in the phase-plane, with the use of Poincaré mapping. This way the behaviour hidden in the time-history plots can be better observed and the block's tendency towards periodicity and multiple orbits can be noted. Furthermore, the phase-plane views reveal highly increased dynamic sensitivity for a slight variation in the initial conditions (initial state not at rest). Orbits that describe the behaviour of rigid rocking block can be symmetric or highly asymmetric; showing in particular that for some values of the excitation frequency, the rocking motion of such block can be asymmetric, thus easier to reach excessive and unstable displacements. An example of the phase-plane view for a free rocking single rigid block with a given angular displacement at the start and the coefficient of restitution lower than 1,0 is shown in Figure 11. Results are obtained using the earlier mentioned developed ad-hoc MATLAB code.

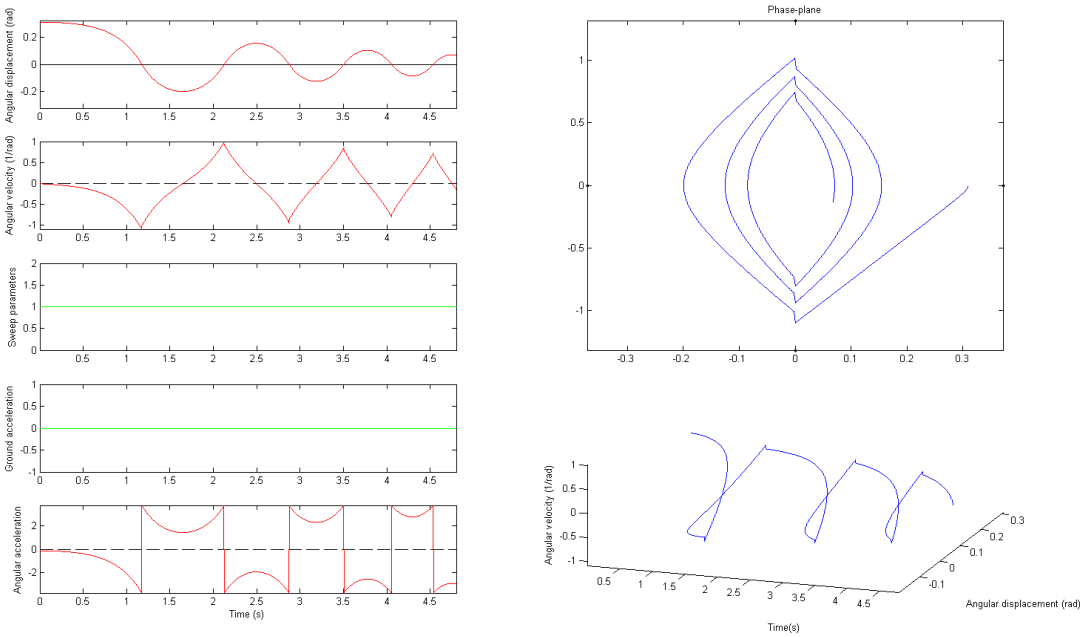

Figure 11. Angular displacements, angular velocity and angular acceleration time-histories compared to phase-plane view

Phase-plane view highlights the discontinuity of rocking motion. Also, it reveals a great variation in the motion amplitude and the angular velocity as a result of a slight variation in initial conditions. A surprising fact is that most authors based their investigations on rigid blocks with initial conditions at rest. This is probably the consequence of complexity of motion even of the most simple rigid block model.

Nevertheless, the issue of initial conditions of rigid block not at rest and the motion following such configuration need to be further researched. An example of a phase-plane view for a single rigid block with initial conditions at rest and the coefficient of restitution lower than 1,0 is shown on Figure 12.

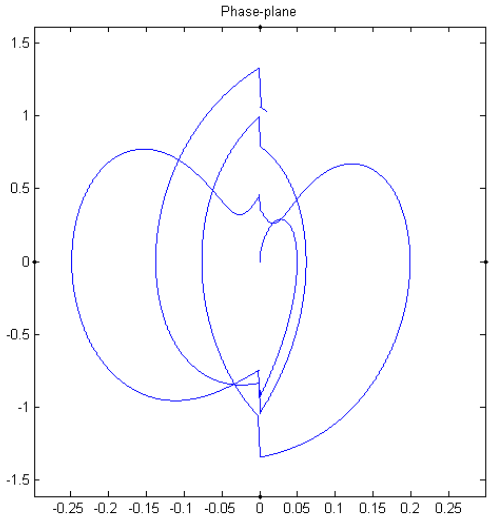

Figure 12. Phase-plane view for 3 seconds of rocking of rigid block under harmonic excitation

The above phase-plane view reveals quasi-symmetric orbits of large amplitude at the beginning of excitation and a tendency for amplitude to decrease further on. Phase-plane views for rocking under harmonic excitation of rigid block with initial angular displacement $\theta_0 = 0{,}005 = 0{,}29°$ and $\theta_0 = 0{,}05 = 2{,}86°$ are shown in Figure 13. Characteristics of the block and amplitude and frequency of ground acceleration are the same as before.

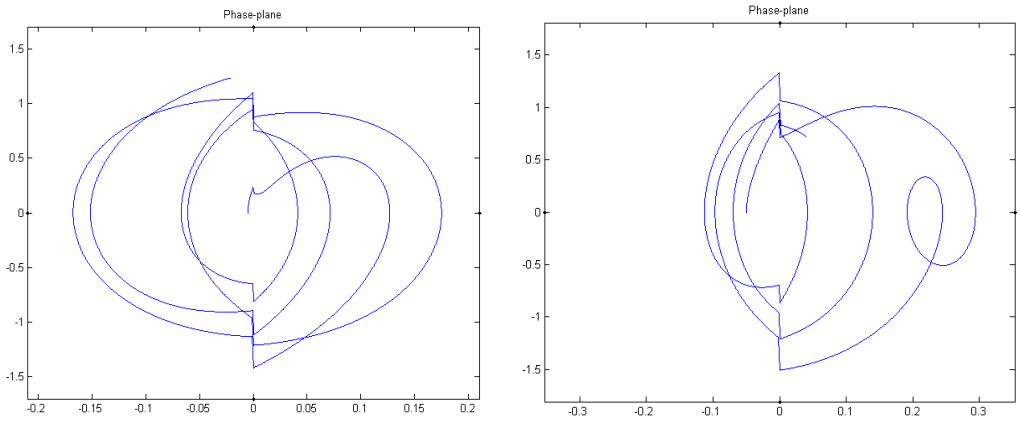

Figure 13. Phase-plane view for 3 second of rocking of rigid block under moronic excitation with initial angular displacement $\theta_0 = 0,005 = 0,29°$ (left) and $\theta_0 = 0,05 = 2,86°$ (right)

Figure 13 (left) reveals notable increase in rocking amplitude and no tendency for decrease in latter during time for a seemingly insignificant small initial rotation, whereas Figure 13 (right) shows even

greater increase in the rocking amplitude (almost 50% decrease) and highly asymmetric behaviour for a further increase of the initial rotation. Since such initial conditions are physically possible and likely to be present in reality, the fact that they strongly affect motion should be given attention to.

Literature review for 2.3. Hogan's analysis of rigid block motion	
Reference	**Conclusions**
Hogan (…)	*Steady-state dynamics* *Periodicity of rocking motion (symmetric and asymmetric orbits)* *Phase-plane view* *Overturning sensibility for varied initial conditions*

2.4. Single rigid block confined between side-walls

There are a small number of papers considering the dynamics of a single block confined between vertical side-walls. This problem is typical in nuclear plants, where there is a high stack of cylindrical blocks placed one a top of the other inside a container. If an earthquake or similar dynamic excitation occurs the dynamic behaviour of such block stacks is highly unpredictable. To be able to analyze this behaviour, one should first be able to analyse the behaviour of a single block in a container, represented by a single block confined between two side-walls in 2D.

Single block of width B and height H is considered. The block is rigid and centre of its mass is considered to be in its geometric centre. Dynamic behaviour of the block is described as in previous sections, with angular displacement θ (positive if block rotates clockwise and negative if block rotates counter-clockwise), angular velocity $\dot{\theta}$ and angular acceleration $\ddot{\theta}$. Side-walls (also referred to as barriers) are also considered to be rigid and cannot suffer any displacements. The situation is sketched in Figure 14.

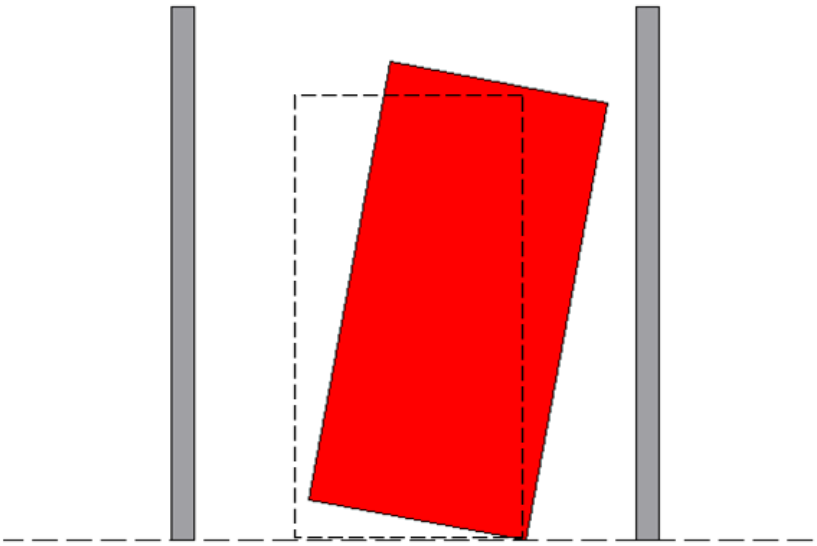

Figure 14. Single rigid block confined between side-walls

The equations of motion (EOM) are the same as Housner's equations of motion during rocking, with the exception of the moment of impact between the block and either the left or the right side-wall.

Since the impact between block and base is considered to be accounted for only by reducing the angular velocity after the impact with the usage of coefficient of restitution, the moment of impact between the block and base is considered to satisfy Housner's EOMs.

The B-W impact (block-wall impact) results in a repulsion force between the two rigid bodies. To simplify the problem, the impact is considered to be only normal, i.e. with its tangential component equal to zero. Since the friction between the block and the base is considered to be high enough that no sliding can occur between these two bodies, and the block cannot penetrate the base, only rotation EOM

needs to be satisfied. The normal-to-wall-surface force which appears in the B-W impact moment results in an additional moment around either point A or point D (depending on the sign of rotation), so the B-W impact time EOM becomes:

$$I_0 \cdot \ddot{\theta} = -W \cdot R \cdot (sign(\theta) \cdot \alpha - \theta) - sign(\theta) \cdot M_{B-W\ impact} \tag{17}$$

There are many ways to treat the impact and determine the value of repulsion force. Further on the impact will be treated as done in the explicit Discrete Element Method (DEM) with penalty terms. The normal contact will be described with gap violation, called the Signorini condition and given as:

$$\begin{aligned} \Delta F_n(i) &= k_n \cdot \Delta n \\ F_n(i) &= F_n(i-1) + \Delta F_n \end{aligned} \tag{18}$$

In the above equation $\Delta F_n(i)$ is normal contact force increment, $F_n(i)$ and $F_n(i-1)$ are total normal contact forces, k_n is a linear penalty coefficient and Δn is depth of penetration.

It is intuitive that a greater value of the penalty coefficient will result in a faster elimination of any penetration between rigid bodies, thus portraying a more correct condition physically. But, a greater value of the penalty coefficient will also artificially increase the angular velocity immediately after the impact which may affect the numerical stability of the numerical model. An example of such event is shown in Figure 15.

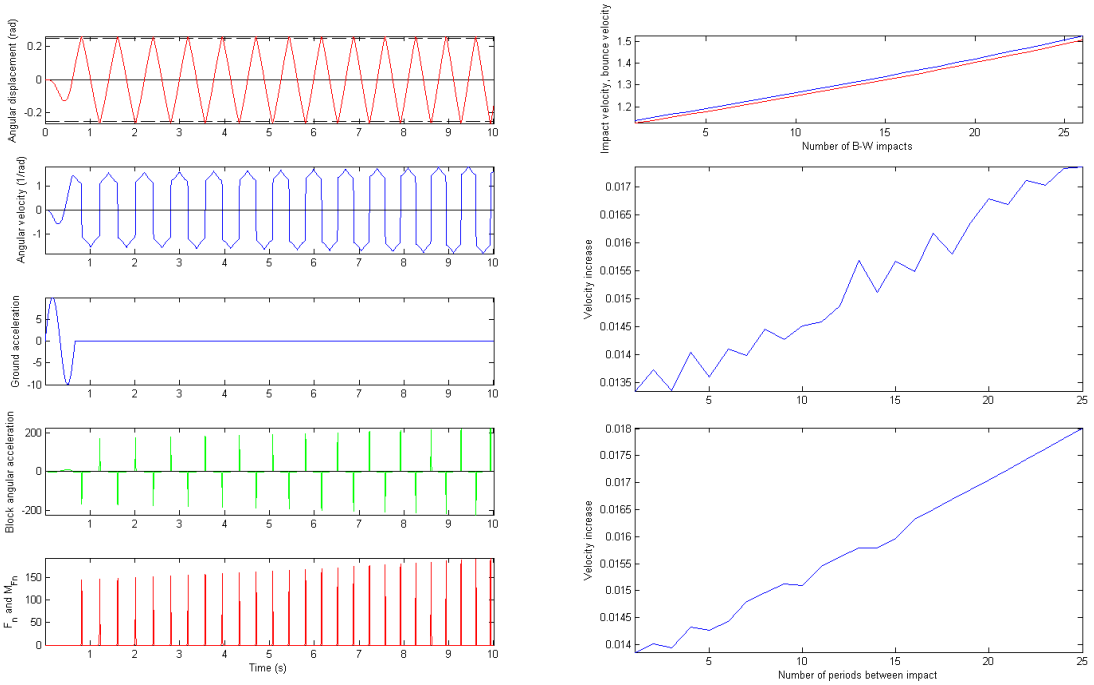

Figure 15. Angular displacements, angular velocity, ground acceleration, angular acceleration and normal contact force time-histories and artificial increase in angular velocity depending on number of impacts for free rocking rigid block confined between side-walls

A single rigid block rocking between two side walls as a result of harmonic excitation shows a less of a pattern in behaviour and it is more difficult to notice the artificial increase in angular velocity. An example is shown in Figure 16.

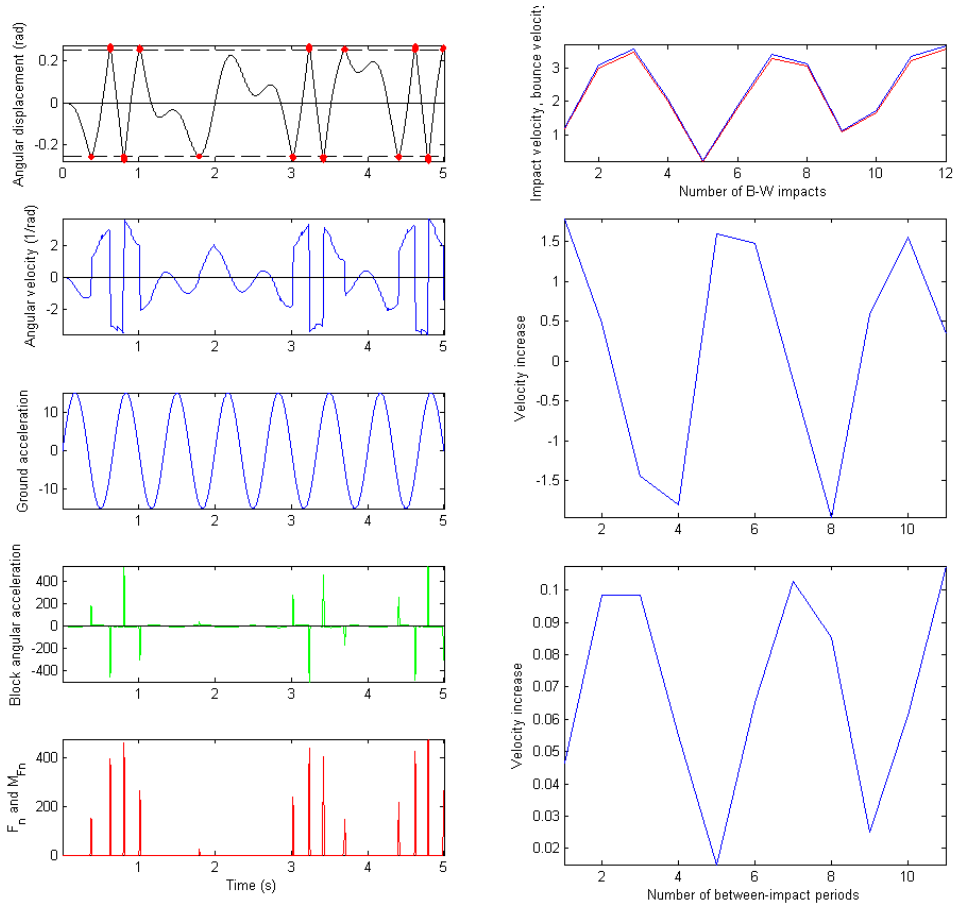

Figure 16. Angular displacements, angular velocity, ground acceleration, angular acceleration and cormal contact force time-histories and artificial increase in angular velocity depending on number of impacts form rigid block confined between side-walls under harmonic excitation

Literature review for 2.3. Hogan's analysis of rigid block motion	
Reference	**Conclusions**
Hogan (1994)	*Steady-state dynamics* *Periodicity of rocking motion (symmetric and asymmetric orbits)* *Phase-plane view*

References

Bićanić, N., Discrete Element Methods, chapter in book

Dimitrakopoulos, G. E., DeJong, M. J., Revisiting the rocking block: closed-form solutions and similarity laws, Proceedings of the Royal Society, 2012

Hogan, S. J., On the dynamics of rigid block motion under harmonic forcing, Earthquake engineering, Tenth World Conference, 1992

Hogan, S. J., On the dynamics of rigid-block motion under harmonic forcing, Proceedings of the Royal Society A, 1989

Hogan, S. J., Rigid block dynamics confined between side-walks, Proceedings of the Royal Society A, 1994

Hogan, S. J., Slender rigid block motion, Journal of Engineering Mechanics, 1994

Hogan, S. J., The many steady state responses of a rigid block under harmonic forcing, Earthquake Engineering and Structural Dynamics, 1990

Housner, W. G., The behaviour of inverted pendulum structures during earthquakes, Bulletin of the Seismological Society of America, 1963

Makris, Roussos, Rocking response and overturning of equipment under horizontal pulse-type motion, report, 1998

Purvance, M. D., Anooshehepoor, A., Brune, J. N., Freestanding block overturning fragilities: Numerical simulation and experimental validation, Earthquake Engineering and Structural Dynamics, 2008

Spanos, P. D., Koh, A.-S., Rocking of rigid blocks due to harmonic shaking, Journal of Engineering Mechanics, 1984

Zhang, J., Makirs, N., Rocking response of free-standing blocks under cycloidal pulses, Journal of Engineering Mechanics, 2001

3. Bi-block structure

A bi-block structure is a structure consisting of two rigid rectangular blocks, where one is on top of the other ('top block' is positioned on top of the 'base block'). When excited by horizontal ground excitation, the bi-block structure starts rocking. There are 4 different patterns which may describe a motion of the bi-block structure at any given time, regarding to the sign of rotation of the base and the top block, θ_1 and θ_2, respectively (Psycharis, 1990, Spanos et al., 2001, Kounadis et al., 2012). The patterns are shown in Figure 17, Figure 18, Figure 19 and Figure 20.

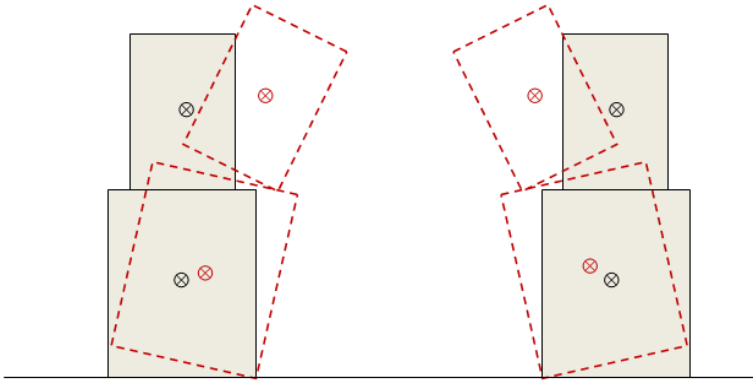

Figure 17. Rocking pattern 1a (left) and 1b (right)

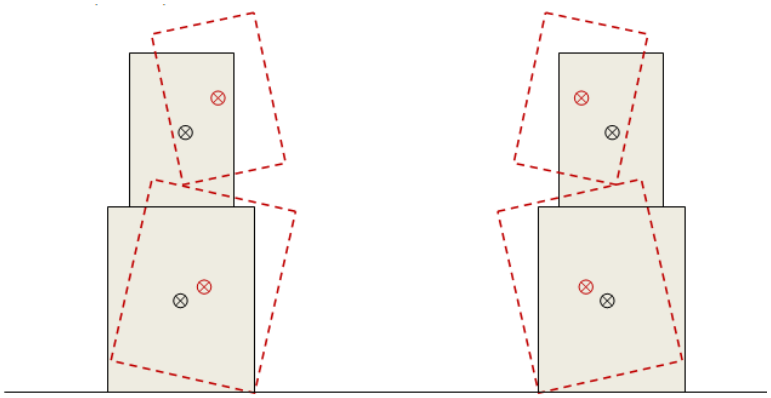

Figure 18. Rocking pattern 2a (left) and 2b (right)

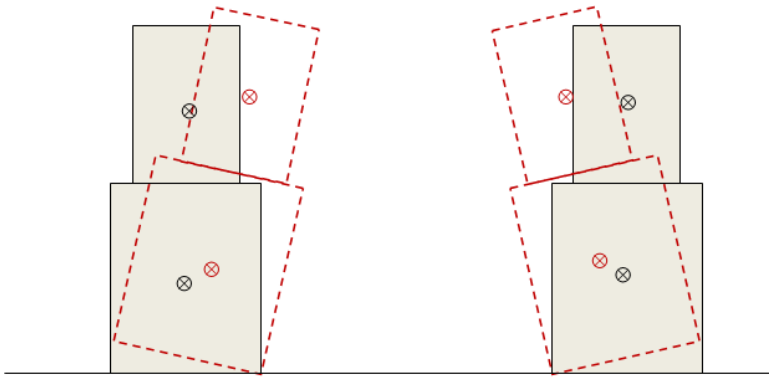

Figure 19. Rocking pattern 3a (left) and 3b (right)

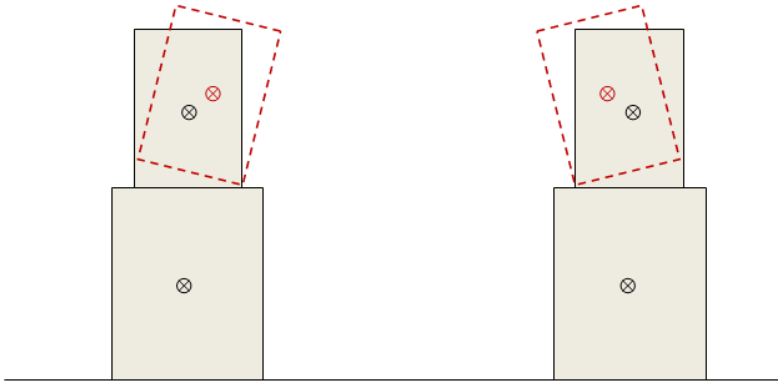

Figure 20. Rocking pattern 4a (left) and 4b (right)

Different equations of motion need to be written for each pattern and for each block. It should be noted that the top block is also subject to translational degrees of freedom, due to the translation of corresponding point on the upper plane of base block, in patterns 1, 2, and 3, about which it rotates. Hence each pattern demands a system of 4 equations to determine 4 unknown variables: $\theta_1, \theta_2, x_2, y_2$.

Another approach to this subject is based on the Lagrangian mechanics. Lagrangian mechanics is based on satisfying the equation (Spanos et al., 2001):

$$\frac{d}{dt}\left(\frac{\partial L}{\partial \dot{\theta}_i}\right) - \frac{\partial L}{\partial \theta_i} = 0 \tag{19}$$

In eq. (19) L is total energy of system, given by:

$$L = K - \Omega \tag{20}$$

In eq. (20) K is the total kinetic energy of the system and Ω is the total potential energy of the system. For the system consisted of two rigid rectangular blocks total kinetic and potential energy are given by:

$$K = \frac{1}{2}\left(I_{01}\dot{\theta}_1^2 + I_{02}\dot{\theta}_2^2 + m_1\dot{u}_1^2 + m_2\dot{u}_2^2 + m_1\dot{y}_1^2 + m_2\dot{y}_2^2\right) \tag{21}$$

$$\Omega = m_1 g y_1 + m_2 g y_2 \tag{22}$$

In eqs. (21) and (22) y_1 and y_2 are coordinates in the y direction of the centre of mass of the base and the top block, respectively. Position coordinates of the base block mass centre depend only on the rotation of the base block. On the other hand, the position coordinates of the top block depend on the rotation of top block and the position of corresponding contact point on the upper plane of base block.

There are four different equations describing the position coordinates of C.M. of top block, depending on the pattern.

Following Kounadis et al. the linearised EOM describing pattern 1 is:

$$\begin{bmatrix} I_{01} + m_2 l^2 & m_2(a_1 h_2 - b_2 \xi) \\ m_2(a_1 h_2 - b_2 \xi) & I_{02} \end{bmatrix} \begin{Bmatrix} \ddot{\theta}_1 \\ \ddot{\theta}_2 \end{Bmatrix} + \begin{bmatrix} -(m_1 h_1 + m_2 a_2) & 0 \\ 0 & -m_2 h_2 g \end{bmatrix} \begin{Bmatrix} \theta_1 \\ \theta_2 \end{Bmatrix} = \begin{Bmatrix} \mp(m_1 b_1 + m_2 \xi) g \mp (m_1 b_1 + m_2 \xi)\ddot{y}_g - (m_1 h_1 + m_2 a_2)\ddot{x}_g \\ \mp m_2 b_2 g \mp m_2 b_2 \ddot{y}_g - m_2 h_2 \ddot{x}_g \end{Bmatrix} \tag{23}$$

Linearised EOM describing pattern 2 is:

$$\begin{bmatrix} I_{01} + m_2 l'^2 & m_2(a_1 h_2 - b_2 \xi') \\ m_2(a_1 h_2 - b_2 \xi') & I_{02} \end{bmatrix} \begin{Bmatrix} \ddot{\theta}_1 \\ \ddot{\theta}_2 \end{Bmatrix} + \begin{bmatrix} -(m_1 h_1 + m_2 a_2) & 0 \\ 0 & -m_2 h_2 g \end{bmatrix} \begin{Bmatrix} \theta_1 \\ \theta_2 \end{Bmatrix} = \begin{Bmatrix} \mp(m_1 b_1 + m_2 \xi') g \mp (m_1 b_1 + m_2 \xi')\ddot{y}_g - (m_1 h_1 + m_2 a_2)\ddot{x}_g \\ \mp m_2 b_2 g \mp m_2 b_2 \ddot{y}_g - m_2 h_2 \ddot{x}_g \end{Bmatrix} \tag{24}$$

Linearised EOM describing pattern 3 is:

$$I_0 \ddot{\theta}_1 - m_{1,2} g h_{1,2} \theta_1 = \mp m_{1,2} b_1 g \mp m_{1,2} b_1 \ddot{y}_g - m_{1,2} h_{1,2} \ddot{x}_g$$
$$\theta_2 = \theta_1 \tag{25}$$

Linearised EOM describing pattern 4 is:

$$\theta_1 = 0$$
$$I_{02}\ddot{\theta}_2 - m_2 g h_2 \theta_2 = \mp m_2 b_2 g \mp m_2 b_2 \ddot{y}_g - m_2 h_2 \ddot{x}_g \tag{1}$$

From the starting position at rest, when the bi-block structure is excited by ground acceleration, it can start rocking following either pattern 3 or pattern 4. Each pattern (subpattern) can be followed by some of the other patterns (subpatterns). The branching diagram showing the possible transitions between patterns is shown in Figure 21.

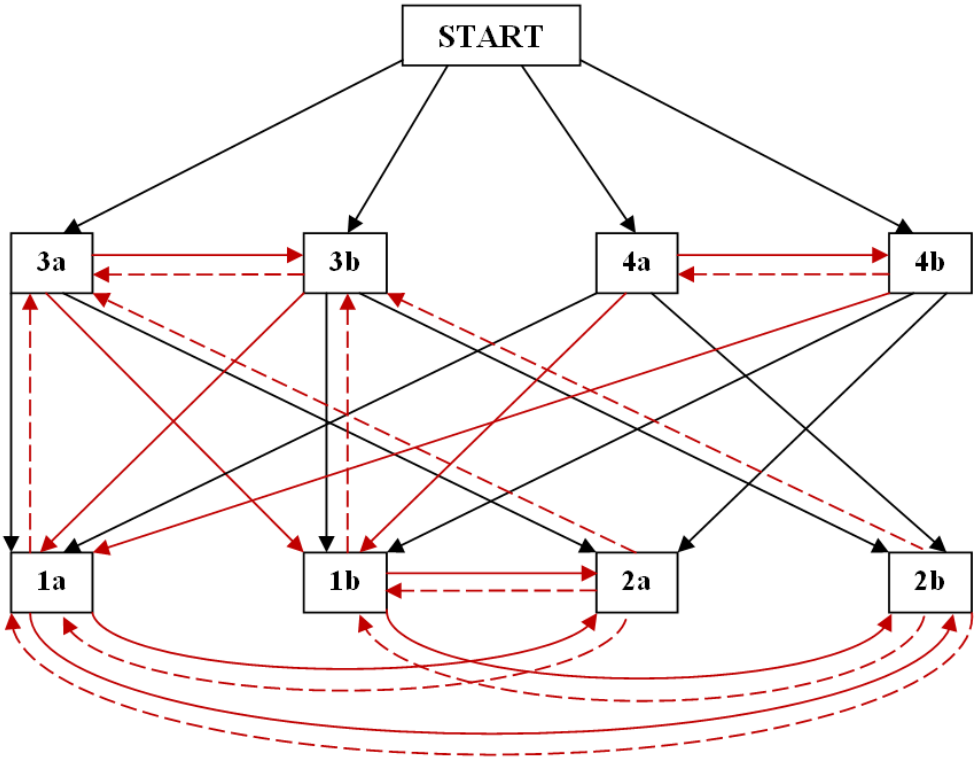

Figure 21. Branching diagram with possible transitions between patterns (subpatterns) based on (Psycharis, 1990, Spanos et al., 2001, Kounadis et al., 2012)

Each transition (each line in Figure 21) corresponds to the fulfilment of a given condition or criterion – the so called branching condition. The transition from one pattern to another can happen with impact between the top and the base block or between the base block and the base (transitions followed by impacts are represented by red lines in Figure 21) or without any impact (represented by black lines in Figure 21).

It can be noted that the overall pattern of behaviour is cyclic, with the exception of the pattern 4 (a and b), and there is a possibility for each pattern to happen again after some time of rocking. It is obvious that the pattern 4 (a and b) can happen only in the beginning or by the transition between patterns 4a and 4b.

From the initial conditions at rest, the bi-block structure can start rocking in either pattern 3 or pattern 4, depending on the ground acceleration values and the characteristics of both blocks. If the given excitation is assumed to be a sine wave ground acceleration without a phase lag, the total intensity of the excitation will progressively grow and the transition condition with a lower threshold will define the starting rocking pattern. There are classes of geometry that can be viewed independently. The boundary between the transition from rest to the pattern 3 and the transition from rest to the pattern 4 for bi-block structure with same constitutive properties and the same height of lower and upper block is shown in Figure 22. Condition which defines the boundary is obtained from linearised EOM.

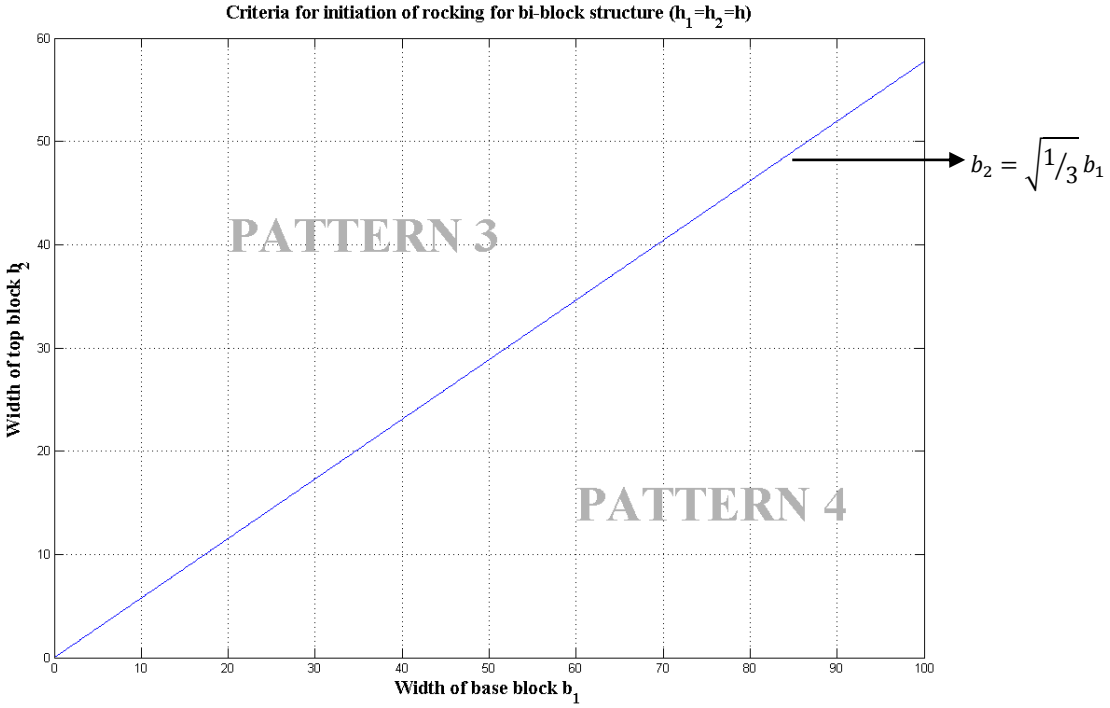

Figure 22. Boundary between transition from rest to pattern 3 and transition from rest to pattern 4 for bi-block structure with same height of lower and upper block

A bi-block structure with the same width of the upper and lower block cannot start rocking in the pattern 4, when excited by sine wave ground acceleration, regardless of the heights of the blocks, as the condition that defines a boundary of transitions to different patterns would require the height of either lower or upper block to be negative, which is physically impossible (**Error! Reference source not found.**). Blue lines on **Error! Reference source not found.** represent the boundary between the transition to pattern 3 and the transition to pattern 4. White area indicates physically possible situations, while the grey area indicates physically non feasible solutions (either negative width or negative height ratio, or both). It can be seen that when the block height ratio is positive, the width ratio asymptotically approaches the value of 1,0 but never reaches it.

Furthermore, the bi-block structure consisting of two blocks with the same dimensions but different masses will also start rocking in pattern 3, regardless of actual value of the masses of blocks.

If the bi-block structure consists of two blocks with same masses but different dimensions, both transitions from rest to rocking with pattern 3 and rocking with pattern 4 are possible, depending on the blocks width and height ratio. When the width of the upper block is half the width of the lower block or smaller, it is not possible for the bi-block structure to start rocking in pattern 4. Boundaries between the transition from rest to pattern 3 and transition from rest to pattern 4 for a bi-block structure consisting of two blocks with the same mass and different width ratios are shown on Figure 23. The area above the boundary line defines the transition from rest to pattern 4, while the area below boundary line defines the transition from rest to rocking in pattern 3, for each width ratio.

It is important to highlight the fact that bi-block structures that are not able to start rocking in pattern 4, i.e. it will never enter rocking in pattern 4 during motion (that can be seen in Figure 21) because the transition to rocking in pattern 4 is possible only from rest or by a transition between pattern 4a and pattern 4b.

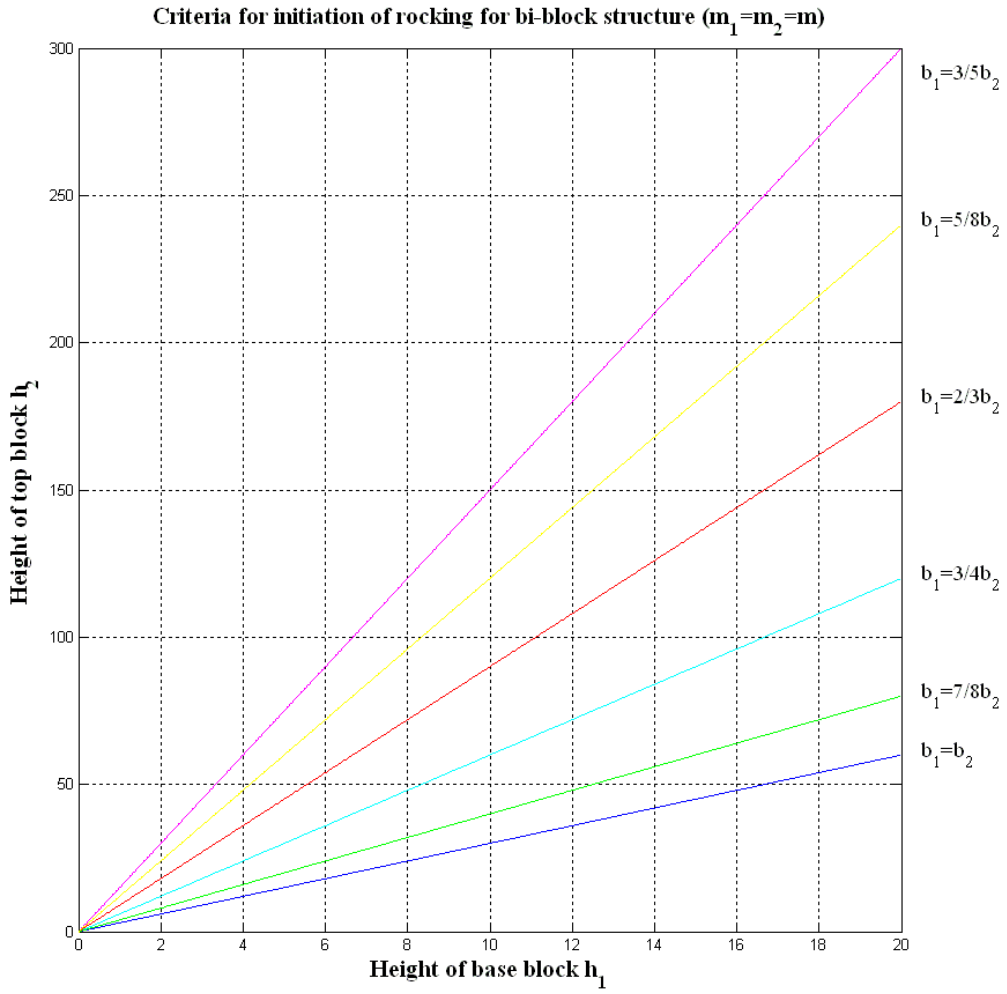

Figure 23. Boundaries between transition from rest to pattern 3 and transition from rest to pattern 4 for bi-block structures with same mass of lower and upper block but different width ratios

The latter case and Figure 23 are associated with bi-block structures consisting of blocks of different materials. The latter case can be better described if the base block and the top block width are the same, but the height ratio and the mass ratio are varied. Since widths are equal it is clear that mass of each block depends on the height of the block and specified density of the block for homogeneous material. Boundaries between the transition from rest to pattern 3 and the transition from rest to pattern 4 are shown on Figure 24. The white area indicates physically possible values, while the grey area indicates non-feasible solutions, i.e. either negative mass or negative height of base or top block. The black line on Figure 24 represents bi-block structures consisting of two blocks of the same material.

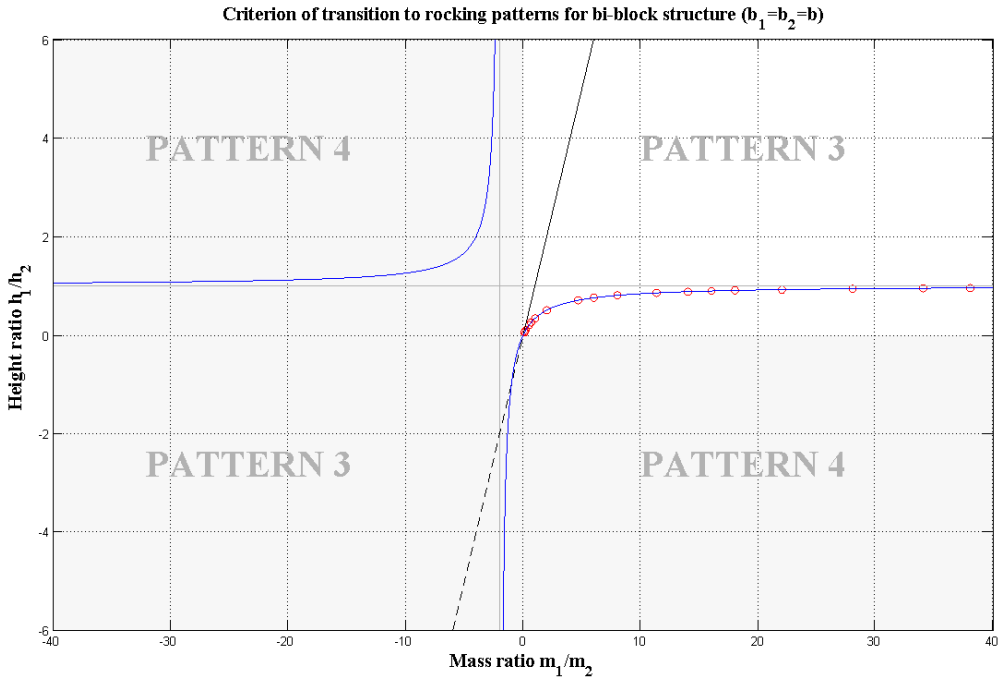

Figure 24. Boundaries between transition from rest to pattern 3 and transition from rest to pattern 4 for bi-block structure with same width of lower and upper block

Part of white area from Figure 24 is shown in Figure 25.

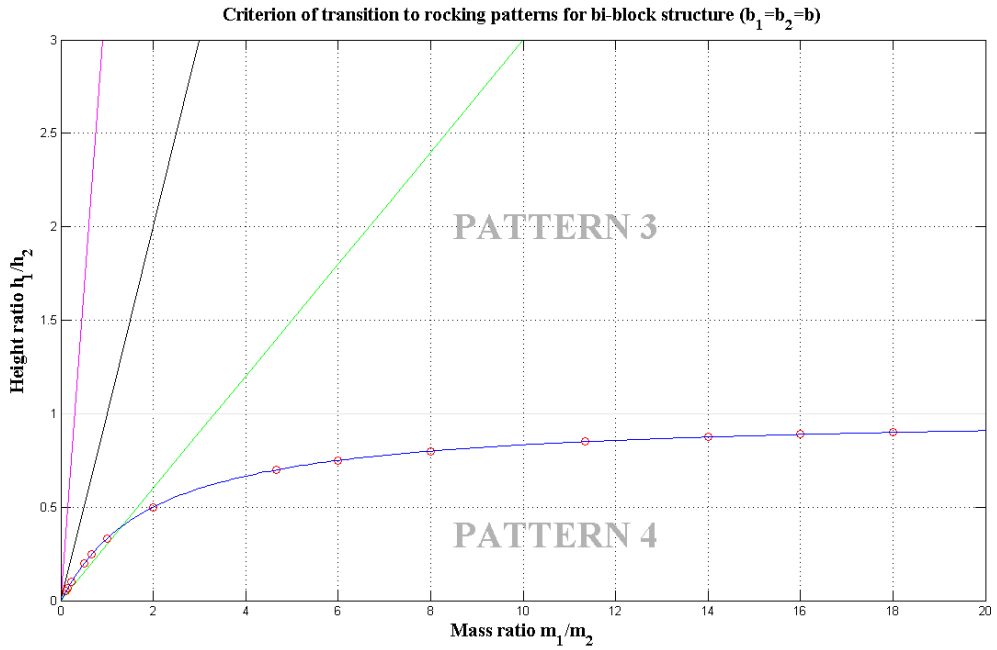

Figure 25. Boundary between transition from rest to pattern 3 and from rest to pattern 4 for bi-block structure with same width of lower and upper block

The black line on Figure 25 again represents two blocks of the same material, while the areas left and right from this line represent a denser lower block or a denser upper block, respectively. The magenta line in Figure 25 represents an example of a concrete block on top of a steel block, while the green line represents a reverse case, of a steel block on top of a concrete block. It is noted that only in the case when the upper block is denser, that the transition from rest to pattern 4 is possible.

Literature review for 3. Bi-block structure	
Reference	**Conclusions**
Spanos, Roussis and Politis (2001)	/
Psycharis (1989)	*Transitions between modes 1, 2, 3 and 4*
Kounadis, Papadopoulos and Cotsovos (2011)	*Conditions for overturning of each block*
Pena, Prieto, Laurencao and Campos-Costa (2006)	/

References

Kounadis, A. N., Papadopoulos, G. J., Cotsovos, D. M., Overturning instability of a two-rigid block system, Z. Angew. Math. Mech., 2012

Spanos, P. D., Roussis, P. C., Politis, N. P. A., Dynamic analysis of stacked rigid blocks, Soil Dynamics and Earhquake Engineering, 2001

Psycharis, I. N., Dynamic behaviour of rocking two-block assemblies, Earthquake Engineering and Structural Dynamics, 1990

Pena, F., Prieto, F., Laurenço, P. B., Campos-Costa, A., Dynamical behaviour of rigid block structures subjected to earthquake motion, Structural Analysis of Historical Constructions, New Delhi, 2006